SINERGI Vol. 24, No. 3, October 2020: 177-188
http://publikasi.mercubuana.ac.id/index.php/sinergi
http://doi.org/10.22441/sinergi.2002.3.002 .

AN FLC-PSO ALGORITHM-CONTROLLED MOBILE ROBOT

Heru Suwoyo[1,3,*], Yingzhong Tian[1,2], Muhammad Hafizd Ibnu Hajar[3]
[1]School of Mechatronic Engineering and Automation of Shanghai University
[2]Shanghai Key Laboratory of Intelligent Manufacturing and Robotics, Shanghai University
266 Jufengyuan Rd, Baoshan, Shanghai 200444, China
[3]Department of Electrical Engineering, Universitas Mercu Buana
Jl. Meruya Selatan, Jakarta 11650, Indonesia
*Corresponding Author Email: heru.suwoyo@mercubuana.ac.id

Abstract -- *The ineffectiveness of the wall-following robot (WFR) performance indicated by its surging movement has been a concerning issue. The use of a Fuzzy Logic Controller (FLC) has been considered to be an option to mitigate this problem. However, the determination of the membership function of the input value precisely adds to this problem. For this reason, a particular manner is recommended to improve the performance of FLC. This paper describes an optimization method, Particle Swarm Optimization (PSO), used to automatically determinate and arrange the FLC's input membership function. The proposed method is simulated and validated by using MATLAB. The results are compared in terms of accumulative error. According to all the comparative results, the stability and effectiveness of the proposed method have been significantly satisfied.*

Keywords: *Wall-Following Robot; Fuzzy Logic Controller; Particle Swarm Optimization; FLC-PSO*

Copyright © 2020 Universitas Mercu Buana. All right reserved.

Received: November 17, 2019 *Revised: March 2, 2020* *Accepted: March 11, 2020* *Published: July 15, 2020*

INTRODUCTION

The main task of WFR is to maintain the distance into the setpoint position safely, commonly-termed as the expected track, when it moves [1, 2, 3, 4, 5, 6]. It is expected to have the ability to make decisions in the form of movements that match the contours of the ever-changing walls. Therefore, it can be declared that the main objective of solving and improving this kind of robot is to involve the proper controller. There are many existing controllers used to keeping the movement of WRF on the expected track, which utilizes the error as the input. The input is then used to decide the required amount of Pulse Width Modulation (PWM) for both the powered wheels. The use of Proportional-Integral-Derivative (PID) and Fuzzy Logic Controller (FLC) [7, 8, 9, 10] can be suggested and recommended as the closed-loop controller [11] suitable for processing the input and giving the feedback to the further decision process.

Different from the principle of the PID controller [8], which utilizes the mathematical calculation, FLC is the type of controller adopting the human thinking and perception [8, 12, 13, 14, 15, 16, 17, 18]. The working principle of FLC can be indicated by the existence of a linguistic term generated from the logical foundation in a different term. This linguistic term is then represented in the form of Membership Function [10][13]. Both the input and output have the membership function connected by the analogy designed by the user. It is called the Rule-Base [12, 17, 18, 19]. It tells that the input is proportional to the output respecting the designer's perception.

The success of using FLC lies in how well the arrangement of MBF is prepared before the system is processed. Traditionally in the case of controlling WFR, it can be arranged manually by estimating both the big the PWM of each wheel when the error is randomly change. Initially, the change of error can be predicted at the beginning. But the properness of the PWM value for each wheel is not that easy to be chosen. Therefore, such manual tuning has been left till nowadays. As the alternative to overcome this lack, there are many special-strategies which adopted from the heuristic-based optimization.

The earliest strategy is a Genetic Algorithm (GA) [20, 21, 22, 23], which utilizes the creation of mutation and crossover in finding the best optimum solution [24]. However, the complexity of using GA has been mentioned.

Besides that, the speed of finding the best solution is too slow, indicated by many generations required to find the answer. As the effort of replacing GA, in this paper, the role of Particle Swarm Optimization (PSO) [7, 13, 24] is

approached to enhance the FLC by automatically arranging the membership function of the input respecting to the output. It is a relatively new optimization method that can be used similarly as GA in finding the optimal solution.

Initially, the kinematic configuration of the real WFR is designed. It is used as the base of movement by ignoring the physic law [11], such as the mass, slippage, and force, or even human interference. It is intended to ease the designer to investigate the movement by only referring to the steering system of WRF. In this case, the real WRF is similarly designed as the wheelchair [18] [25], which contains two powered wheels and a freewheel. The steering principle can be concerned with the diversity of the speed of the powered wheel mounted on the backside since the freewheel gives no effect to the movement. Relating to the used controller, FLC, the starting needs from this analogy is the output, which can be represented by the value of PWM in the form of the membership function.

Moreover, in order to make a robot to be autonomous, the WRF is equipped with three distance sensor HC-SR04. They are mounted on the left, right, and front side-body, which are further used to detect any obstacle or wall on the left, right, and the front side of the robot body, respectively. When it is closed to the front wall and referred to the front sensor, the robot turns right with 90° translational movement when the robot senses there is the wall on the left side. Contrary, WFR turns left with a 90° translational movement when the front sensor senses the obstacle, and the previously detected wall is on the right side. Meanwhile, the data transferred from the left and right sensors is directly processed by FLC. It is firstly converted as the values of error and classifying as the input membership function. Simply, the input membership function is adopted from the left or right sensor, and the output membership function is the PWM prepared for both the powered wheels. As noted, the optimization is only intended to arrange the input membership function instead of both the input and output.

Once the completeness mentioned above is prepared, the performance of WRF is simulated based on the proposed method, Fuzzy Logic Controller, enhanced by Particle Swarm Optimization. Henceforth, it is termed as FLC-PSO. In order to evaluate the effectiveness, stability, and robustness, it is compared with the performance of the WRF. Since there are two types of errors, which are positive and negative, the negative errors are converted to be positive. It is then used to add the recorded positive error.

Thus, those different performances are compared in the term of accumulative error or the total positive error for the whole robot movement. The fastest performance of WRF can be determined based on the achieved goal position in the same duration. Meanwhile, the stability can be directly seen from the graphical representation. Moreover, by observing the speed of PSO in finding the best solution, the robustness of the proposed method can be observed. Finally, based on all the comparative results, the proposed method has been effectively and significantly improving the performance of WFR.

The rest of this paper is organized as follows; Materials and Methods are described in Section 2, Experimental results are described and discussed in Section 3, and Conclusions are presented in section 4.

METHOD

The WFR is the robot assigned to follow the wall by utilizing the distance sensor mounted on the body of the robot. In order to improve the performance of WFR, the closed-loop controller, FLC is used. Essentially, FLC processes the input membership function and makes decision with respect to the proper output based on the rule-based system [3, 4, 15, 16, 17, 19, 26, 27]. There have been many products applying the principle of FLC, such as in the case of adjusting the air conditioner based on the actual temperature, pressing the pedal of an automatic car based on the crowds around, and adjusting the heat based on the food maturity placed on the barbeque cooker. As the helper for making the decision, FLC is essential can be done by manually arranging the input membership function. However, it is no longer proper for the application with the random change of the input, such as WFR. For this reason, the use of PSO is approached in this project. By using PSO, the arrangement of the input membership function can be offline-determined [24, 28, 29]. Therefore, as an effort to optimize the FLC, the simulation is required. For simulation, the movement principle should be involved based on the robot platform (see Figure 2). The principle of movement can be easily depicted and then used as the base by only attracting it as the kinematic configuration shown in Figure 1.

The kinematic configuration shown by Figure 1 is adopted from the wheeled mobile robot consist of two layers of the body, and the main controller named as *Arduino Mega* [29, 30, 31,32].

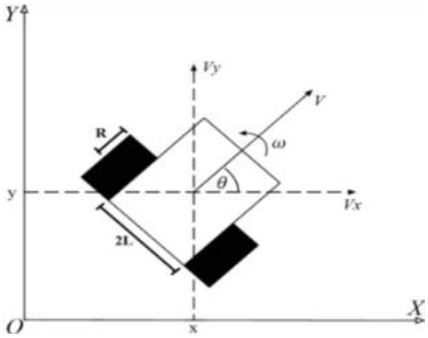

Figure 1. Kinematic Configuration

It has three wheels, which is an unpowered wheel and two powered wheels completed with the rotary encoder, three distance sensors placed on a specific side, as clearly mentioned before. It is also completed with a fan connected to the DC motor. This WFR is actually used for the implementation purpose of the fire-fighting robot [29] [30]. The appearance of this robot is shown in Figure 2.

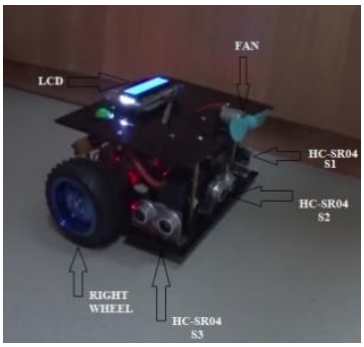

Figure 2. Wheeled Mobile Robot

As a common way for quickly observing the movement based on the kinematic configuration shown in Figure 1, the law of differential steering system is approached in this project. First, considering that the robot is placed in a flat environment, there will be two different positions, which are the spatial and orientation pose [2] [11]. The spatial pose (x, y) represents the position of the robot with respect to x and y coordinate when the model is modelled 2D. Meanwhile the orientation θ represents the angle formed by the robot heading to x coordinate of the global frame. Simply, the orientation pose is commonly-called as the heading. Up to this point, the current pose $p_{(t)}$ of the wall-following robot can be mathematically expressed as follows

$$p_{(t)} = [x_{(t)} \quad y_{(t)} \quad \theta_{(t)}]^T \tag{1}$$

Then by considering, there are two types of velocity named linear v and angular velocity ω affecting the movement. The transition movement of the robot can be calculated as in Equation (2).

$$\acute{p} = \begin{bmatrix} \acute{x} \\ \acute{y} \\ \acute{\theta} \end{bmatrix} = \begin{bmatrix} cos\theta_{(t)} & 0 \\ sin\theta_{(t)} & 0 \\ 0 & 1 \end{bmatrix} \begin{bmatrix} v \\ \omega \end{bmatrix} \tag{2}$$

Next by applying the transition movement (2) to the current pose $p_{(t)}$, the future pose $p_{(t+1)}$ is then calculated as

$$p_{(t+1)} = p_{(t)} + \acute{p} \tag{3}$$

Note that the robot only needs the linear and angular velocity in order to update the pose of the robot respect to the time scale t. Therefore, since the command sent to the motor driver is in the form of value PWM, the angular velocity should be firstly concerned. In this project, all the values of PWM are converted into the angular velocity of the right wheel ω_r and left wheel ω_l. It is done by recording the rotation of each wheel caused by specific values through the rotary encoder. Then, by referring to the angular velocity of all the independently driven wheel, the right wheel ω_r and left wheel ω_l, the complete Equation for a differential steering [6, 33, 34] system can be sequentially summarized as follows

$$v = \frac{(\omega_r + \omega_l)R}{2} \tag{4}$$

$$\omega = \frac{(\omega_r - \omega_l)R}{2L} \tag{5}$$

$$\omega_r = \frac{v + \omega L}{R} \tag{6}$$

$$\omega_l = \frac{v - \omega L}{R} \tag{7}$$

Where R and L are the radius of the driven wheel and half of the length of the robot body, respectively.

The kinematic configuration shown by Figure 1, it is the initial configuration when the wheeled mobile robot is placed on the free-obstacle environment. Therefore, in order to start the simulation, the representation should firstly be redesigned. Since there is no change of the cause of the movement, then the graphical representation of the kinematic configuration of WFR can be depicted in Figure 3. It is noted that, since the movement is adopted from the linear and angular velocity generated from the PWM for each DC motor, the Equation (1)-(7) can still be used.

However, to start the simulation, a model of the mobile robot shown in Figure 1 should be remodeled. Therefore, by referring to the differential steering system, the model of WFR with $R = 3.5cm$ and $L = 10cm$ as depicted in Figure 3.

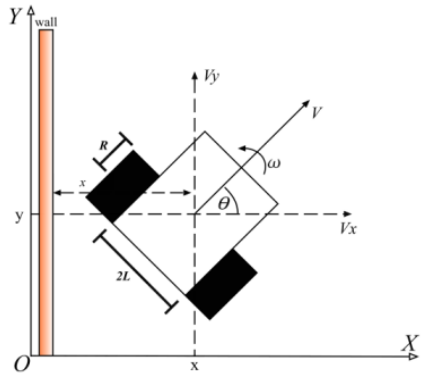

Figure 3. Model of The Wall-Following Robot

According to the principle of WFR, the error would be considered equal to zero while the robot successfully moves on the predetermined path. The robot moves closer to this expected path when it is far from the wall by turning left or right, depending on the location of the wall. The common issue of the WFR movement is wave-movement due to the improper speed of each wheel when it is turned.

Consequentially, the error would always change because of the turn actions. Therefore, as an effort to present the threshold for analyzing the performance of WFR, the error is accumulated. It is done by quadrating all the types of error which can be calculated as follows

$$te = \sum_{it=0}^{max} e(it)^2 \tag{8}$$

where te refers to the total of the error and $e(it)$ is the current error calculated based on the difference between the value of the predetermined dd and actual distance ad. Simply, the error can be mathematically expressed as

$$e(t+1) = dd - ad(t) \tag{9}$$

Up to this point, it is clear that there are two contradictive values of the error under time integration.

The Wall-Following Robot Controlled by FLC Optimized by PSO

Although the wall is flat, the turn action of the robot makes the data received by the sensor will always random. Since the speed is adjusted based on these data, it is hard to know the effective values for each wheel. Therefore, the role of FLC is adopted in this project. By using FLC, it can be adjusted automatically even when the change of the input is rapidly changed. FLC is inspired by human experts [7, 8, 14, 35] who make decisions by involving the step of the fuzzification, the rule base, and defuzzification, as described in Figure 4.

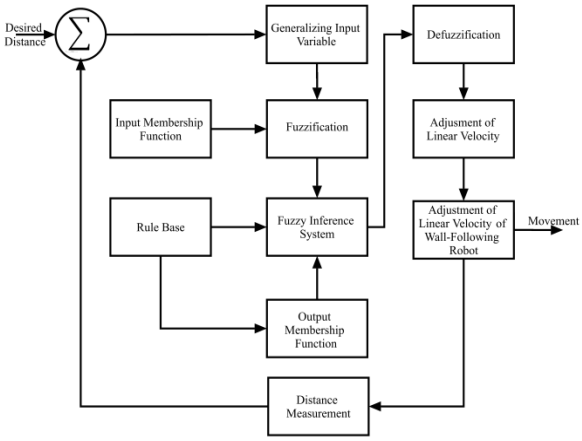

Figure 4. Flowchart of FLC for WFR

It is clear that based on the kinematic configuration in Figure 1 with known R and L, then two input variables on mobile robot movement are linear v and angular velocity ω. The adjustment of the linear and angular velocities affects the movement of the robot when tracing the wall. And in this project, the angular velocity ω is given manually based on the expected orientation. Meanwhile, the linear velocity v is adjusted by referring to the output value of the FLC. Furthermore, since the input of distance is used as core-base in the FLC process, the FLC only produces the linear velocity v.

In this experiment, the input distance is obtained from an HCSR04 mounted on the left side of the robot body. The readable distance value of the sensor is initially converted directly to the error value by using Equation (9). Then this error value would be processed on membership classification as input. To do so, it is assuming that the sensor reads the value on the ranges of $3cm$ up to $23cm$ and if every $1cm$ represents the error value respecting to the predetermined ideal distance[4]. Then it is clear to classify possible error as the input membership function as shown in Figure 5. It is noted that the ideal distance is set as $13cm$.

Regarding Figure 5, the grouping step is done by only giving label on every subset range, i.e., the error value -1 to 0 represents “close” robot distance, -0.5 to 0.5 representing “medium” and 0 to 1 representing the robot distance when “far” from the wall.

Once arranging the input membership function is completed, the output setting can be sufficiently done in this fuzzification step. This stage is a semi-free stage to estimate the range speed of the robot. The robot has the lowest speed of $0\ dm/s$ and the fastest speed of $0.3\ dm/s$.

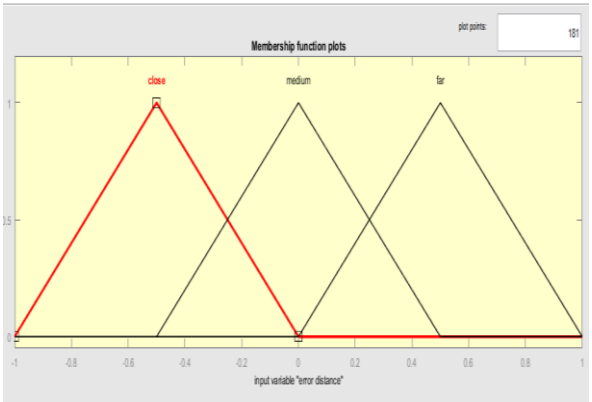

Figure 5. Input Membership Function

Respectively, all the arrangement shown in Figure 5 is proportional to the arrangement depicted in Figure 6.

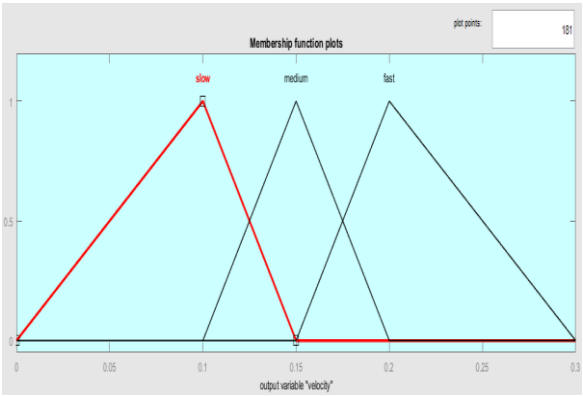

Figure 6. Output Membership Function

According to Figure 6, it is obvious that all the linguistic terms of slow, medium, and fast refer to close, medium, and far, respectively.

Once the fuzzification step is done, the values of input and output membership function are then correspondingly connected by referring to the form of if-then of Fuzzy Logic Controller. It refers to the Mamdani version, which is used as the base to design the rule base connection. It is adapted from the analogy that the robot quickly moves away from the wall when it is near the wall, moves forward with the normal speed when it is on the ideal path, and moving closer to the wall with the lower speed to the wall. Therefore, after applying all the described steps above, the FLC system leads to the defuzzification process. In this project, the centroid defuzzification [10, 36, 37] is used, in which its general Equation is known as follows

$$z_0 = \frac{\int \mu_i(x)xdx}{\int \mu_i\,(x)dx} \tag{10}$$

where z_0 is the defuzzified output, μ_i is a membership function, and x is the output variable.

By using FLC, the proper speed based on the distance of the robot to the wall is efficiently and effectively obtained. Finally, the performance is significantly improved as there is no much wobble on its movement (see Figure 12).

However, it is done by only manually arranging the input membership function. Thus, the enhancement can still be conducted. It is done by using the PSO as the manner to optimize the FLC.

PSO is inspired by the social foraging behavior of some animals, such as the flocking behavior of birds and the schooling behavior of fish [7, 13, 24]. The correlation between PSO and FLC is depicted in Figure 7. As can be seen in Figure 7, the PSO is connected to the system for gaining the proper value for all of the subsets on the input membership function. It leads to an automatic arrangement.

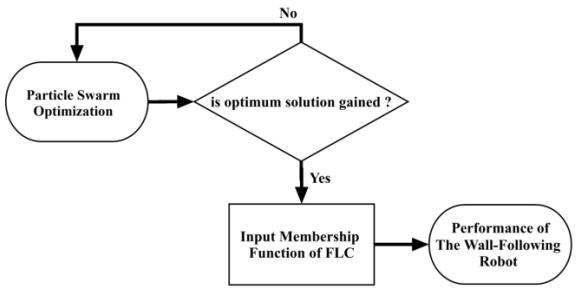

Figure 7. The Flowchart of PSO and FLC in Controlling the Wall-Following Robot

In this experiment, the values in each subset of the input membership function are represented by the particles. These particles are assumed to consist of randomly generated positions and velocities by promoting the limits of the range. The condition is an early stage in the use of PSO [4, 7, 13]. Then evaluate the process for the determination of $PBest$ and $GBest$ using the fitness function. It is clear that the fitness function is the total error te, which represents the performance of WFR.

Meanwhile, $PBest$ and $Gbest$ stands for Best Position and Global Best, which represent the best particle value and the best fitness, respectively. After this process, these two variables are stored to represent the best solution in every generation. The generation or the number of repetitions in the searching process is predetermined with a value of 200 repetitions. Once the best solution for each generation is achieved, it is then used as the reference for the next step. Contrary, the system restarts from the beginning until the better solution completed. By

doing so, the representative solutions are improved generation-by-generation. The solution in the last generation provides the best solution indicated by the presence of the lowest fitness value. Since the position of each particle representing the affecter to the fitness function, the PSO finds the optimum solution by applying the velocity to the certain particle given the previous position of particles. It is mathematically calculated by using the general Equation of PSO, as shown in Equation (11) and (12).

$$v_{j+1}^{i} = wv_j + c_1 r_1 \left(pbest^{i} - x_j^{i}\right) + c_2 r_2 \left(gbest_j - x_j^{i}\right) \quad (11)$$

$$x_{j+1}^{i} = x_j^{i} + v_{j+1}^{i} \quad (12)$$

where v_j^i is the velocity of ith particle at the jth iteration, x_j^i is the current solution of ith particle at the jth iteration. r_1 and r_2 represent the random number uniformly generated, satisfying the range of $0 \sim 1$. Meanwhile, c_1 and c_2 value is self-confidence (cognitive) factor and swarm-confidence (social) factor, respectively. w is inertia factor that takes linearly decreasing values downward from 1 to 0 according to the predefined number of iterations as recommended by Haupt, 2004 [13, 24, 29]. Figure 8 is presented to ease the description of this analogy. It shows the complete process of PSO used in this experiment.

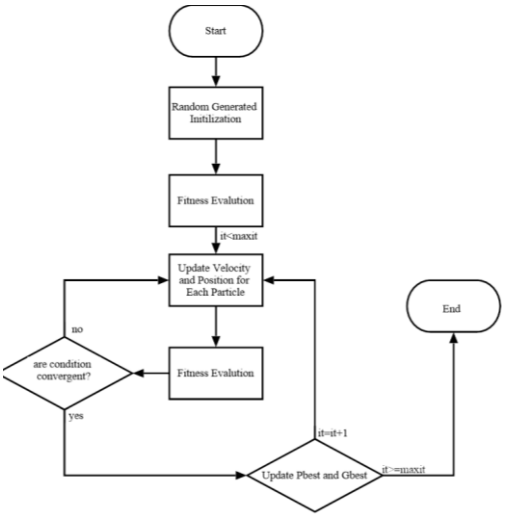

Figure 8. PSO's Flowchart

As the closing part of Section 3, the best result of WFR controlled by FLC-PSO has the total error, as shown in Figure 9. This figure shows that the changes in all the fitness values in each generation within the looping process or $maxit$up to 200 times. Finally, the last gained solution is considered, and its affecter is used to arrange the input membership function of FLC (see Figure 11).

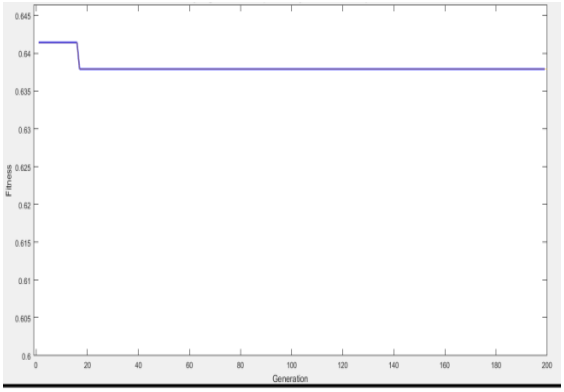

Figure 9. The Change of The Fitness Function

As discussed earlier that each generation consists of the solution for subset in the input membership function, which are represented by $MBF1$, $MBF2$ and $MBF3$ for *"close," "medium,"* and *"far"* (see Figure 10). Figure 10 represents the normal arrangement of the input membership function without any optimization manner. Therefore, by connecting the relationship of Figure 10 and the affecter at the last generation shown by Figure 9, the arrangement of the input membership function of FLC optimized by PSO are respectively expressed by $MBF1 = -0.49643$, $MBF2 = -0.472$ and $MBF3 = 0.39386$ with the fitness value is equal to 0.63791.

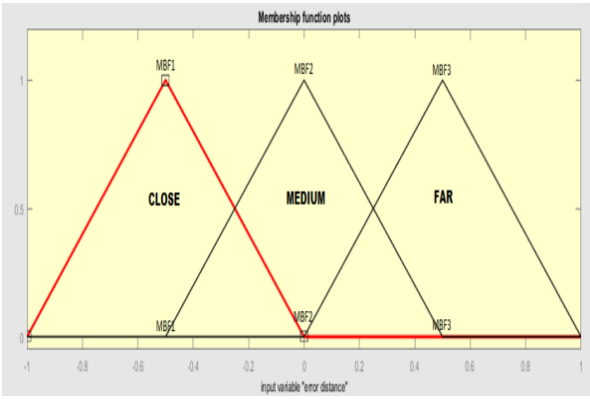

Figure 10. The Optimization Target of The Wall-Following Robot Controlled by FLC

RESULT AND DISCUSSION

By performing the several stages discussed in Section 3, the arrangement of the input membership function becomes, as shown in Figure 11.

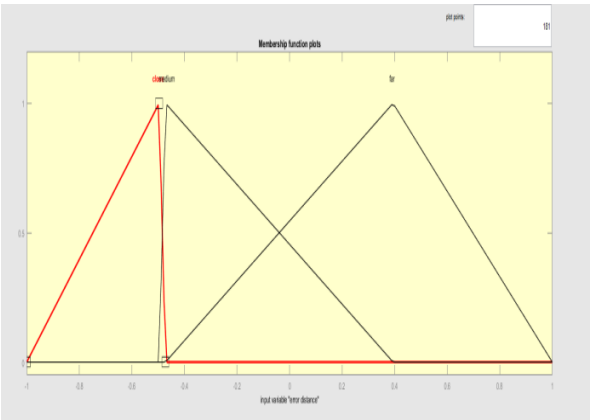

Figure 11. Optimized-Input Membership Function

Figure 11 explains that the input membership function of the manual settings shown in Figure 5 has been changed. Each parameter changes automatically. Next, to observe the striking difference between the proposed and the common method, this paper presents two results of WFR simulation that are controlled by using manual settings of FLC and FLC optimized by PSO. Graphically, they are respectively depicted in Figure 12 and Figure 13. These figures represent the WFR performance simulated by placing the robot beside the wall on the left side at the starting point. The wall is assumed flat length up to $2.5m$ which is a bend and back straight along $3.5m$ and a curve back straight along $2.5m$ are available

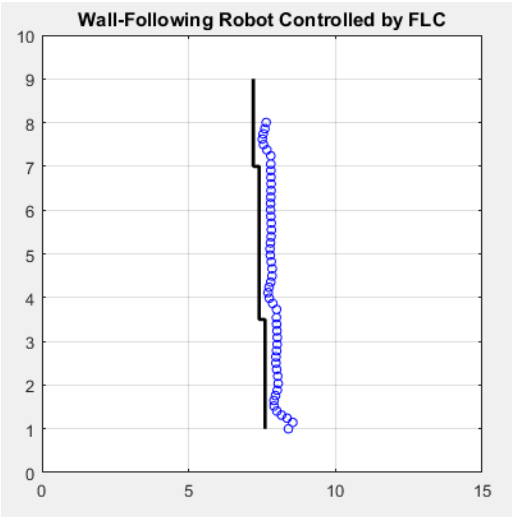

Figure 12. The Performance of WFR Controlled by FLC

Figure 12 shows the performance of WFR controlled by FLC with the normal adjustment to the input membership function. Initially, the robot is placed on the coordinate $x = 8.4, y = 1, and\ \theta = \pi/4$ referring to the kinematic configuration on the 2D Cartesian. Additionally, the robot performs the 50 times moving step, and the latest position is shown on $0.146069943m$ far away from the starting point.

The graphical results shown in Figure 12 and Figure 13 are used as the base to validate the stability and effectiveness of the proposed method.

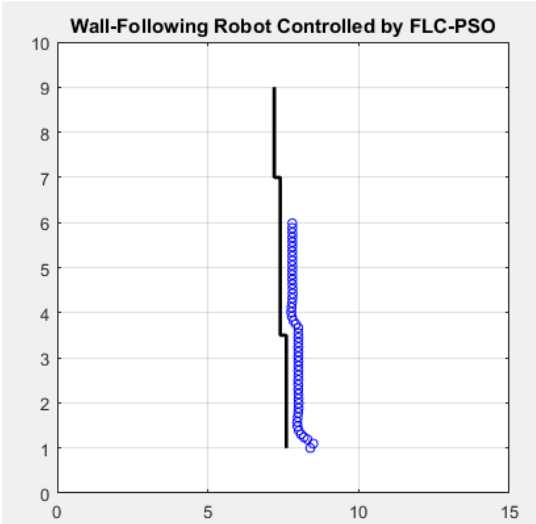

Figure 13. The Performance of WFR Controlled by FLC-PSO

Figure 13 depicts the performance of the WFR controlled by FLC-PSO. The simulation is also begun by placing the WFR on the same starting point with 50 times of moving step. BY comparing both performances (Figure 12 and Figure 13), the normal arrangement of the input membership function is able to make the WFR faster than the proposed method. However, it gives much wobble of the movement. It does not overcome the main objective of WFR, which is reducing the wave motion. Contrary, the WFR controlled by FLC-PSO (in Figure 13) shows the stable movement with no much wobble when it is following the wall. Therefore, it can be stated that the proposed method is better than the traditional method in terms of stability.

The speed is not concerned as the parameter of consideration. The reason is, the dynamic movement of the WFR significantly depends on the flatness of the wall. In this experiment is assumed that the wall is flat. Therefore, when the robot faces the wave wall, the WFR with the fast movement will diverge to the expected performance. Thus, the validation method is only referring to the smaller error of different performances of the WFR. For this reason, Table 1 is presented in this paper to show the detailed comparison of the error in cm.

Table 1. The Error and Latest Position of The Performance of The Wall-Following Robot Controlled by FLC

The WFR Performance Controlled by FLC-Normal Setting			The WFR Performance Controlled by FLC-PSO		
Step	**Error (cm)**	**Latest Pose (m)**	**Step**	**Error (cm)**	**Latest Pose (m)**
1	-4	0.14606994	1	-4	0.09642614
2	-5.460699	0.24302586	2	-4.964261	0.19332111
3	-3.521581	0.31270675	3	-3.026362	0.2397104
4	-1.619049	0.40417552	4	-1.874919	0.30283099
5	-0.008476	0.52101942	5	-0.91979	0.38205463
6	0.9374044	0.64588188	6	-0.177101	0.47718661
7	0.9426959	0.75885652	7	0.2604066	0.57936926
8	0.4131813	0.88227195	8	0.3508898	0.68067759
9	-0.168535	1.03521386	9	0.218983	0.78190867
10	-0.484499	1.20005622	10	0.0413782	0.88494252
11	-0.34559	1.35718728	11	-0.071435	0.98912305
12	0.0350587	1.50366153	12	-0.092989	1.0933626
13	0.288159	1.64364406	13	-0.055757	1.19737808
14	0.2636209	1.7829708	14	-0.007396	1.30122824
15	0.0628797	1.92929998	15	0.0215563	1.40497498
16	-0.129997	2.08407392	16	0.0253927	1.50869747
17	-0.178658	2.24024872	17	0.0142133	1.61247282
18	-0.077147	2.39257731	18	0.0010377	1.71631902
19	0.0589272	2.54021022	19	-0.006342	1.8202043
20	-1.884126	2.72837616	20	-0.006881	1.92409175
21	-1.939566	2.86583752	21	-0.003587	2.02796281
22	-0.644594	2.98733481	22	-1.3E-05	2.13181665
23	0.5336664	3.11425983	23	0.0018495	2.23566146
24	0.9427419	3.23480951	24	0.0018563	2.33950619
25	0.6210753	3.35355836	25	0.000896	2.44335566
26	0.0613277	3.49456861	26	-6.79E-05	2.54720993
27	-0.376562	3.65704211	27	-2.000533	2.66260001
28	-0.426383	3.8181332	28	-2.000494	2.74418204
29	-0.123079	3.96933909	29	-1.184456	2.82202945
30	0.1992792	4.11189435	30	-0.40579	2.91311513
31	0.2870069	4.25124382	31	0.1336452	3.0142497
32	0.1481596	4.39428685	32	0.3388421	3.11624079
33	-0.057112	4.54606022	33	0.270689	3.21733436
34	-0.169545	4.70220147	34	0.0994152	3.31976407
35	-0.124958	4.85631966	35	-0.039218	3.42368371
36	0.0056925	5.00580567	36	-0.090874	3.52795955
37	0.0990896	5.15206565	37	-0.070426	3.63205015
38	0.0949267	5.29829843	38	-0.023131	3.73595408
39	0.022476	5.44725782	39	0.013457	3.8397346
40	-0.048225	5.59910302	40	0.0254597	3.94346043
41	-0.06529	5.75155377	41	0.0184805	4.04721466
42	-0.02853	5.9025788	42	0.0052727	4.15103812
43	0.0207721	6.05175636	43	-0.004321	4.25491306
44	-1.957948	6.24079283	44	-0.007059	4.35880166
45	-1.977581	6.37602507	45	-0.004815	4.46267876
46	-0.653693	6.49651726	46	-0.001148	4.56653809
47	0.5377226	6.62317836	47	0.001352	4.67038533
48	0.9517099	6.74351147	48	0.0019483	4.77422963
49	0.6281808	6.8619101	49	0.0012463	4.87807737
50	0.064775	7.00265505	50	0.0002347	4.98193013

According to Table 1, the WFR controlled by FLC-PSO is almost always giving the smaller error for each step. It can be analyzed from all the values of the error, which is closed to zero. Besides that, it is almost always smaller compared to the normal one. It might the cause why the WFR controlled by FLC-PSO can smoothly following the wall. Additional to that, the achieved positions for every step are not much different from each other when the previous error is small. It is the base to state that although the WFR controlled by FLC-PSO tends to be slower than the traditional ones, the speed is not that slow as the WFR. In order to easily see the comparative error of the different performances, Figure 14 is presented.

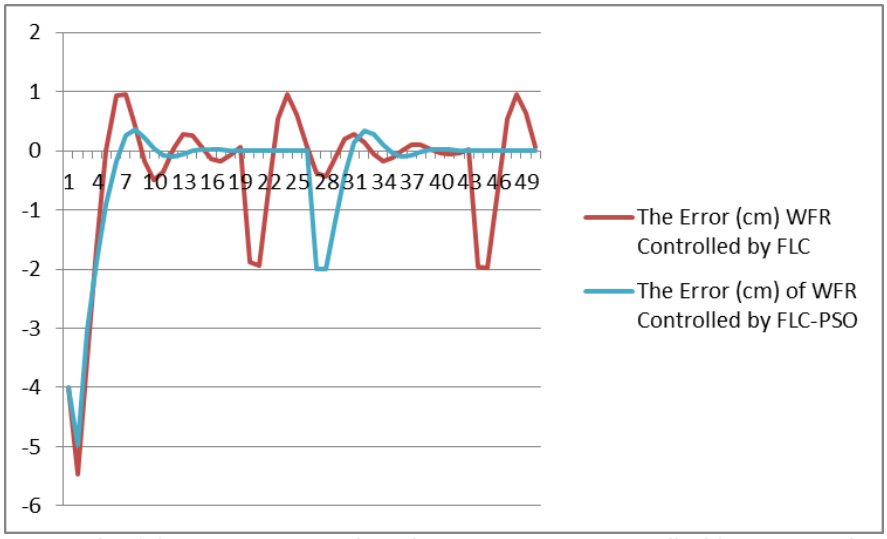

Figure 14. Graph of the Error Comparison between WFR Controlled by FLC and FLC-PSO

At this point and according to Figure 14, it can be stated that the WFR controlled by FLC-PSO is better than the traditional one in terms of stability.

Lastly, the optimization process of PSO can be done only by offline methods. Therefore, in order to operate the PSO as the online method applicable for tuning the FLC, a certain approach is involved in this experiment. It allows using the PSO directly when FLC controls the WFR. Therefore, as the final stage of this project, all the simulation results are then forwarded to the real robot platform (Figure 2). In order to apply it without any degradation to the performance of the WFR, the fast PSO is approached. It is an effective way to manipulate the obtained solution from simulation to real implementation. Essentially, it requires the only rearrangement of the range for each particle predetermined at the first step of PSO.

CONCLUSION

Adding the closed-loop controller of FLC on the WFR has been effectively leading the robot to work successfully. However, the performance still has a problem shown by the wobble movement. It is because of the random input causing the dynamic error. Once the main objective of using FLC lies in the arrangement of the membership function, the FLC can be enhanced by properly arrange the input or output membership function. In this experiment, the use of FLC is to produce the optimal value for the linear velocity v when the angular velocity ω is predefined. This arrangement is impossible conducted by manual tuning because of the unpredictable input.

Consequently, a manner based on PSO is proposed to enhance FLC controlling the WFR. Henceforth, it called an FLC-PSO algorithm. Since it is a type of heuristic optimization method, which operates based on the predicted future act, the PSO can only be clearly observed and validated by doing simulation. The simulation is done by adopting the differential steering system with the kinematic configuration of the used WFR. Accordingly, the proposed method has been significantly improving the performance of WFR by adequately arranging the input membership function of FLC. The smaller error proves it with smooth movement. Therefore, it can be concluded that the effectiveness and stability of the proposed method are satisfied.

ACKNOWLEDGMENT

The research was supported by Special Plan of Major Scientific Instruments and Equipment of the State (Grant No.2018YFF01013101), National Natural Science Foundation of China (61704102), the IIOT Innovation and Development Special Foundation of Shanghai (2017- GYHLW01037), Project named “Key Technology Research and Demonstration Line Construction of Advanced Laser Intelligent Manufacturing Equipment” from Shanghai Lingang Area Development Administration, Universitas Mercu Buana, Jakarta, Indonesia.

REFERENCES

[1] T. L. Chung, T. H. Bui, S. B. Kim, M. S. Oh, T. T. Nguyen, and K. Words, “Wall-Following Control of a Two-Wheeled Mobile Robot,” *KSME International Journal*, vol. 18, no. 8, pp. 1288–1296, August 2004. DOI: 10.1007/BF02984242

[2] Y. Z. Chang, R. P. Huang, and Y. P. Chang, "A simple fuzzy motion planning strategy for autonomous mobile robots," *IECON 2007 33rd Annual Conference of the IEEE Industrial Electronics Society*, Taipei, 2007, pp. 477–482. DOI: 10.1109/IECON.2007.4460225

[3] A. Budianto et al., "Analysis of artificial intelligence application using back propagation neural network and fuzzy logic controller on wall-following autonomous mobile robot," *2017 International Symposium on Electronics and Smart Devices (ISESD)*, Yogyakarta, Indonesia, 2017, pp. 62–66. DOI: 10.1109/ISESD.2017.8253306

[4] U. Farooq, A. Khalid, M. Amar, A. Habiba, S. Shafique, and R. Noor, "Design and low cost implementation of a fuzzy logic controller for wall following behavior of a mobile robot," *International Conference on Signal Processing System (ICSPS 2010)*, Dalian, 2010, vol. 2, pp. V2-740-V2-746. DOI: 10.1109/ICSPS.2010.5555781

[5] R. A. Dain, "Developing Mobile Robot Wall-Following Algorithms Using Genetic Programming," *Applied Intelligence*, vol. 8, no. 1, pp. 33-41, 1998. DOI: 10.1023/ A:1008216530547

[6] C. F. Juang, Y. H. Jhan, Y. M. Chen, and C. M. Hsu, "Evolutionary Wall-Following Hexapod Robot Using Advanced Multiobjective Continuous Ant Colony Optimized Fuzzy Controller," *IEEE Trans. Cognitive and Development System*, vol. 10, no. 3, pp. 585–594, September 2018. DOI: 10.1109/TCDS.2017.2681181

[7] S. Agrawal and V. Shrivastava, "Particle swarm optimization of BLDC motor with fuzzy logic controller for speed improvement*," 8th International Conference on Computing, Communication and Network Technologies (ICCCNT),* New Delhi, India, 2017, pp. 1-5. DOI: 10.1109/ICCCNT.2017.8204006

[8] E. Elsheikh, M. A. El-Bardini, and M. A. Fkirin, "Dynamic path planning and decentralized FLC path following implementation for WMR based on visual servoing," *2016 3rd MEC International Conference Big Data and Smart City (ICBDSC)*, Muscat, Oman, 2016, pp. 1-7. DOI: 10.1109/ICBDSC.2016.7460359

[9] R. Woo, E. J. Yang, and D. W. Seo, "A fuzzy-innovation-based adaptive Kalman filter for enhanced vehicle positioning in dense urban environments," *Sensors* (Switzerland), vol. 19, no. 5, March 2019. DOI: 10.3390/ s19051142

[10] Y. Bai and D. Wang, *Fundamentals of Fuzzy Logic Control - Fuzzy Sets, Fuzzy Rules and Defuzzifications BT - Advanced Fuzzy Logic Technologies in Industrial Applications*, pp. 17–36, 2006. DOI:10.1007/978-1-84628-469-4_2

[11] L. H. Prayudhi, A. Widyotriatmo, and K. S. Hong, "Wall following control algorithm for a car-like wheeled-mobile robot with differential-wheels drive," *The 2015 International Conference on Control, Automation and Systems (ICCAS)*, Busan, South Korea, 2015, pp. 779–783. DOI: 10.1109/ICCAS.2015.7364726

[12] K. Al-Mutib, M. Faisal, M. Alsulaiman, F. Abdessemed, H. Ramdane, and M. Bencherif, "Obstacle avoidance using wall-following strategy for indoor mobile robots," *2016 2nd IEEE International Symposium on Robotics and Manufacturing Automation (ROMA)*, Ipoh, Malaysia, 2016, pp. 1–6. 017. DOI:10.1109/roma.2016.7847817

[13] M. Collotta, G. Pau, and V. Maniscalco, "A Fuzzy Logic Approach by Using Particle Swarm Optimization for Effective Energy Management in IWSNs," *IEEE Transaction on Industrial Electronics*, vol. 64, no. 12, pp. 9496–9506, December 2017. DOI:10.1109/ TIE.2017.2711548

[14] J. Berisha, X. Bajrami, A. Shala, and R. Likaj, "Application of Fuzzy Logic Controller for obstacle detection and avoidance on real autonomous mobile robot," *2016 5th Mediterranean Conference on Embedded Computing (MECO 2016)*, Bar, 2016, pp. 200-205. DOI: 10.1109/MECO.2016. 7525740

[15] A. S. Handayani, T. Dewi, N. L. Husni, S. Nurmaini, and I. Yani, "Target tracking in mobile robot under uncertain environment using fuzzy logic controller," *International Conference on Electrical Engineering, Computer Science and Informatics (EECSI),* Yogyakarta, Indonesia, September 2017, pp. 1-5. DOI: 10.1109/EECSI.2017.8239079

[16] C. H. Chinag and C. Ding, "Robot navigation in dynamic environments using fuzzy logic and trajectory prediction table," *International Conference on Fuzzy Theory Its Applications (iFUZZY 2014)*, Kaohsiung, Taiwan, 2014, pp. 99–104. DOI: 10.1109/iFUZZY.2014. 7091240

[17] M. R. H. Al-Dahhan and M. M. Ali, "Path tracking control of a mobile robot using fuzzy logic," *13th International Multi-Conference on Systems, Signals and Devices (SSD),* Leipzig, Germany, 2016, pp. 82-88. DOI: 10.1109/SSD.2016.7473656

[18] Y. T. Lee, C. S. Chiu, and I. T. Kuo, "Fuzzy wall-following control of a wheelchair," *IFSA-SCIS 2017 - Jt. 17th World Congress of*

International Fuzzy Systems Association and 9th International Conference on Soft Computing Intelligence System, Otsu, Japan, 2017. DOI:1 0.1109/IFSA-SCIS.2017. 8023223

[19] F. Lachekhab and M. Tadjine, "Goal seeking of mobile robot using fuzzy actor critic learning algorithm," *Proceeding 2015 7th International Conference on Modelling, Identification and Control (ICMIC)*, Sousse, Tunisia, 2015, pp. 1-6. DOI: 10.1109/ICMIC. 2015.7409370

[20] N. Lu, Y. Gong, and J. Pan, "Path planning of mobile robot with path rule mining based on GA," *Proceeding of the 28th Chinese Control and Decision Conference (CCDC),* Yinchuan, China, 2016, pp. 1600–1604. DOI: 10.1109/ CCDC.2016.7531239

[21] X. Wang, B. Song, Y. Liang, and Q. Pan, "EM-based adaptive divided difference filter for nonlinear system with multiplicative parameter," *International Journal of Robust and Nonlinear Control*, vol. 27, no. 13, pp. 2167-2197, 2017. DOI: 10.1002/rnc.3674

[22] M. S. White and S. J. Flockton, "Adaptive Recursive Filtering Using Evolutionary Algorithms," In: Dasgupta D., Michalewicz Z. (eds). *Evolutionary Algorithms in Engineering Applications*, Springer., Berlin, Heidelberg, 1997. pp. 361–376, 1997. DOI: 10.1007/978-3-662-03423-1_21

[23] T. Duckett, "A genetic algorithm for simultaneous localization and mapping," *Proceeding IEEE International Conference on Robotics and Automation*, Taipei, Taiwan, 2003, vol. 1, pp. 434-439. DOI: 10.1109/ ROBOT.2003.1241633

[24] F. Fei, H. Hongjie, and G. Zhongtong, "Application of genetic algorithm PSO in parameter identification of SCARA robot," *Proceeding of 2017 Chinese Automation Congress (CAC 2017),* Jinan, China, January 2017, pp. 923–927. DOI: 10.1109/CAC. 2017.8242898

[25] C. Caceres, J. M. Rosario, and D. Amaya, "Approach of Kinematic Control for a Nonholonomic Wheeled Robot using Artificial Neural Networks and Genetic Algorithms," *2017 International Conference and Workshop on Bioinspired Intelligence (IWOBI)*, Funchal, Portugis, 2017, pp. 1-6 DOI: 10.1109/IWOBI.2017.7985533

[26] C. Chen, H. Du, and S. Lin, "Mobile robot wall-following control by improved artificial bee colony algorithm to design a compensatory fuzzy logic controller," *2017 14th International Conference on Electrical Engineering/ Electronics, Computer, Telecommunications, and Information Technology (ECTI-CON)*, Phuket, Thailand, 2017, pp. 856-859. DOI: 10.1109/ECTICon. 2017.8096373

[27] M. Boujelben, D. Ayedi, C. Rekik, and N. Derbel, "Fuzzy logic controller for mobile robot navigation to avoid dynamic and static obstacles," 2017 14th International Multi-Conference on Systems, Signals and Devices (SSD 2017), Marrakech, Marocco, 2017, pp. 293–298. DOI: 10.1109/SSD.2017. 8166963

[28] Á. Odry, R. Fullér, I. J. Rudas, and P. Odry, "Kalman filter for mobile-robot attitude estimation: Novel optimized and adaptive solutions," *Mechanical Systems and Signal Processing*, vol. 110, pp. 569-589, September 2018. DOI: 10.1016/j.ymssp. 2018.03.053

[29] A. Adriansyah, H. Suwoyo, and Y. Tian, "Improving wall-following robot performance using PID-PSO Controller," *Jurnal Teknologi*, vol. 81, no. 3, pp. 119-126, May 2019. DOI: 10.11113/jt.v81.13098

[30] H. Suwoyo, C. Deng, Y. Tian, and A. Adriansyah, "Improving a wall-following robot performance with a PID-genetic algorithm controller," *International Conference on Electrical Engineering, Computer Science, and Informatics (EECSI)*, Malang, Indonesia, October 2018, pp. 314-318. DOI: 10.1109/ EECSI.2018.8752907

[31] H. Suwoyo, Y. Tian, W. Wang, M. M. Hossain, L. Li," A MAPAEKF-SLAM Algorithm with Recursive Mean and Covariance of Process and Measurement Noise Statistic," *SINERGI,* vol. 24, no. 1, February 2020, pp. 37-48. DOI: 10.22441/sinergi. 2020.1.006

[32] H. Suwoyo, Y. Tian, and M. H. Ibnu Hajar, "Enhancing the Performance of the Wall-Following Robot Based on FLC-GA," *SINERGI,* vol. 24, no. 2, June 2020, pp. 141-152. DOI: 10.22441/sinergi. 2020.2.008

[33] A. Karambakhsh, M. Yousefi Azar Khanian, M. R. Meybodi, and A. Fakharian, "Robot navigation algorithm to wall following using fuzzy Kalman filter," *IEEE International Conference on Control and Automation (ICCA),* Santiago, Chile, 2011, pp. 440–443. DOI: 10.1109/ICCA.2011.6138043

[34] Fahmizal and C. H. Kuo, "Development of a fuzzy logic wall following controller for steering mobile robots," 2013 International Conference on Fuzzy Theory and Its Applications (iFUZZY), Taipei, Taiwan, 2013. pp. 7–12. DOI: 10.1109/iFuzzy.2013. 6825401

[35] M. Ghiasvand and K. Alipour, "Formation control of wheeled mobile robots based on fuzzy logic and system dynamics," *2013 13th Iranian Conference on Fuzzy Systems (IFSC),* Qazvi, Iran, 2013, pp. 1–6. DOI: 10.1109/IFSC.2013.6675674

[36] S. Nandu, N. Nagori, and A. Reshamala, "Autonomous Robot Navigation using Fuzzy Logic," In: *S. Sataphathy and S. Dad. (Eds.). Proceeding of First International Conference on Information and Communication Technology for Intelligent System*, vol. 51, Springer, Cham, 2016. DOI: 10.1007/978-3-319-30927-9_44

[37] X. Li and D. Wang, "Behavior-based Mamdani fuzzy controller for mobile robot wall-following," *2015 International Conference on Control, Automation and Robotics (ICCAR 2015),* Singapore, 2015, pp. 78-81. DOI: 10.1109/ICCAR.2015.7166006